COBEM 2021 26th International Congress of Mechanical Engineering
ABCM Associação Brasileira de Engenharia e Ciências Mecânicas
November 22-26, 2021, Virtual Congress, Brazil

COBEM2021-0148
DEVELOPMENT OF AN EXPERIMENTAL METHODOLOGY FOR REAL-TIME THERMAL ERRORS COMPENSATION OF MACHINED WORKPIECES IN A 5-AXIS MACHINING CENTER IN NON-CONTROLLED TEMPERATURE ENVIRONMENT CONDITION

Marcelo Otávio dos Santos
Éd Claudio Bordinassi
Adalto de Farias
Instituto Mauá de Tecnologia, Praça Mauá, 01 – São Caetano do Sul/SP – 09580-900
FEI - Centro Universitário da Fundação Educacional Padre Saboia de Medeiros – Av. Humberto de Alencar Castelo Branco, 3972, S. Bernardo do Campo/SP – 09850-901
marcelo.santos@maua.br / mosantos@fei.edu.br
ecb@maua.br / edbordinassi@fei.edu.br
adalto.farias@maua.br / afarias@fei.edu.br

Rodrigo Lima Stoeterau
Gilmar Ferreira Batalha
Escola Politécnica da Universidade de São Paulo - Av. Prof. Luciano Gualberto, 380 – São Paulo/SP - 05508-010
rodrigo.stoeterau@usp.br
gfbatalh@usp.br

Abstract. *The objective of this work was to carry out machining tests on engine heads to estimate the contribution of the heat generated in the machining in the thermal error of the part, also evaluating the contribution of ambient heat in the part heating and its consequences for the precision loss in the machining and finally develop a model for compensation of the thermal errors and to implement it. The machine used to carry out the tests was a GROB 5-axis universal machining center. For the machining tests, a total of 45 parts were used. The temperature in the room was 20ºC during all the tests carried out, which were divided into three stages. All machined parts in stages 1 and 2 had their temperature measured by a probe and some of their machined characteristics measured in CMM. After analyzing the results obtained, a methodology for correcting thermal errors was proposed in stage 3. After implementing the correction model, 15 parts were machined and measured to verify its effectiveness. The proposal for thermal compensation of the part was based on the calculation of thermal expansion coefficients from the results obtained during stages 1 and 2, and inserted directly into CNC program for each machined characteristic. Analyzing the results obtained after the thermal compensation it is possible to affirm that the developed methodology was effective, reducing the thermal errors between 62% and 96%.*

Keywords: *Thermal error, 5-axis machining center, machining tests, thermal error compensation.*

1. INTRODUCTION

In a shop floor external heat sources arise from the environment in which the machine is located, such as neighboring machines, the opening or closing of workshop doors, the cyclical variation in the ambient temperature throughout the day and night, and the different temperatures between seasons (Abdulshahed, Longstaff, and Fletcher 2015). Ramesh, Mannan, and Poo (2003) also point out that geometric errors exist in machine tools due to their basic design, inaccuracies that arise during the manufacturing and assembly phases, and because of wear of the machine components themselves.

Until recently, machine tool manufacturers had passed the responsibility for managing such errors to the users of machine tools by specifying certain environmental temperature requirements and/or non-productive procedures for preheating the machine (Xu, 2017).

The level of machining accuracy that can be achieved by error compensation is highly dependent on both the accuracy of the machine itself, and the method chosen to determine the correlation between the different errors. The former is related solely to the design and manufacture of the machine, while the latter is highly dependent on a knowledge of the influence of these errors on the machining accuracy, which may be difficult to implement in mathematical models. The two main approaches to improving machine tool accuracy are complete cancellation and compensation of errors (Miao *et al*., 2013).

Achieving error cancellation would involve building an accurate machine during the design and manufacturing phases in such a way that errors can be kept to a minimum. Good practice for handling these errors includes better attribution of stiffness, adequate damping, careful selection of materials, a symmetrical structure, and efficient cooling systems, and these approaches have been widely adopted (Zhu, Ni and Shih, 2008). Although the cancellation of errors by perfecting the basic structure of the machine or controlling the environmental working conditions is generally accepted as the best way to eliminate errors, this has two primary disadvantages. Firstly, it is impossible to eliminate all the errors solely through design and manufacturing techniques, and secondly, machining costs increase exponentially as the level of precision increases (Turek, Modrzycki, and Jędrzejewski, 2010). A major concern is that these mechanisms tend to be expensive, and software-based error compensation techniques are therefore widely used instead.

Several researchers have sought to identify the critical points in a machine tool at which the temperature needs to be periodically monitored, and various methods have been used to analyze the data obtained to develop an adequate method of compensation (Chang *et al*., 2005). Measuring the temperature and component errors is only a first step towards the goal of improving the accuracy of machine tools (Delbressine *et al*., 2006); another important step is the correction of these errors in real time, so that their effects on the machining accuracy can be minimized.

Mareš *et al*. (2020) implemented a scheme for thermal compensation of the main internal and external heat sources that affect the structure of a five-axis machine tool using transfer functions. The inputs to the compensation algorithm were data from native temperature sensors used primarily for diagnostic purposes on the machine. These authors were able to obtain a significant reduction in thermal errors in the three linear (X, Y and Z) directions of the machine during a verification test lasting more than 60 h. In addition, a thermal specimen was machined to verify the industrial applicability of the developed approach, and the results of their transfer function model were satisfactory compared to a multiple linear regression compensation model.

Liu *et al*. (2017) explored the advantages of a physics-based model over a data-driven model, and physically modeled the thermal errors of a ball screw and the motor of a TC500R vertical machining center with a FANUC API 0i MD open architecture command. The thermal errors were measured using a Renishaw Company XL80 laser interferometer.

Li, Zhao, and Lu (2020) reported that the feed/drive systems of a CNC machine tool were characterized by several heat sources and a high rate of time-varying heat generation for each heat source. However, they found that previous studies had paid little attention to the time-varying rate of heat generation for each heat source, making it difficult to accurately predict the temperature rise and thermal error in the ball screws of the feed units. In their work, Li *et al*. (2020) integrated the FEM method with Monte Carlo simulation to determine the heat generation rate of each heat source in the drive/supply system. In this way, they obtained the ratio of each heat source to the total heat generation rate of the system as a function of operating time and proposed a numerical prediction model for the thermal error in the ball screw of the feed unit.

1.1 Objective

Machining tests were carried out with the following objectives:

- To estimate the contribution of heat generated when machining a workpiece with minimum quantity lubrication (MQL) in the thermal error of machining center.
- Estimate the machined hole position thermal error in a part subject to temperature variation. This test was implemented to evaluate the contribution of ambient heat to the workpiece heating and its consequences for the loss of precision in machining. A common problem in plants located in regions of high temperature, without an air-conditioned room.
- In the experiments carried out in this work, the machine operated at a controlled temperature of 20oC, but the parts to be machined were subjected to initial temperatures higher than room temperature.
- Develop a workpiece thermal error compensation model and implement it on the CNC program.

2. METHODS AND MATERIALS

2.1 Description of the experimental step

The machine tool used to carry out the machining experiments was a 5-axis GROB universal machining center, model G550AB (Figure 1).

Figure 1. Machining center G550AB installed in the technological center of B. GROB of Brazil company.

In order to carry out the MQL machining tests, 45 cylinder heads in aluminum AlSi6Cu4 were used (Figure 2). The room temperature was at 20 °C ± 1 °C during all machining tests performed, which were divided into three steps (Table 1):

- **Step 1**: 20 pieces were divided into 4 batches of 5 pieces each (batches #1 to #4), where each batch would be heated to a certain temperature (20 ºC, 25 ºC, 30 ºC and 35 ºC, respectively), to be machined later. In this step, the parts' temperatures were measured after machining the first cutting tool and after machining the last cutting tool, at the end of machining. The temperature measurement points on the parts were points #3 and #4, which are shown in Figure 2.
- **Step 2**: Two more batches of 5 pieces each (batches #5 and #6) were machined. Parts from batch #5 are at an initial temperature of 20 ºC and parts from batch #6 are initially at 30 ºC. In this step, temperature measurements took place after each tool change (total of 13 tool changes). Measurements at points #3 and #4 occurred for all thirteen tool changes, while points #1 and #2 were measured only at the last four tool changes.
- **Step 3**: Based on the position deviation results obtained after measuring the parts in a three-dimensional coordinate measuring machine (CMM), a model for calculating the thermal compensation factor of the part was proposed, which when inserted into the CNC of the machine, will compensate its thermal errors. Three other batches of parts (lots #7, #8 and #9), totaling 15 previously heated parts, were machined for verification and validation of the proposed method.

Table 1 shows the distribution of parts for each batch, the respective temperature of the parts entering into the machining center and the condition of the machining test.

Table 1. Distribution of machined parts in 3 steps.

Step	Batch	Number of machined parts per batches	Entry temperature of parts into the machine	Test condition
1	#1	5 parts – 1 to 5	20 ºC	no compensation
1	#2	5 parts – 6 to 10	25 ºC	no compensation
1	#3	5 parts – 11 to 15	30 ºC	no compensation
1	#4	5 parts – 16 to 20	35 ºC	no compensation
2	#5	5 parts – 21 to 25	20 ºC	no compensation
2	#6	5 parts – 26 to 30	30 ºC	no compensation
3	#7	5 parts – 31 to 35	25 ºC	with compensation
3	#8	5 parts – 36 to 40	30 ºC	with compensation
3	#9	5 parts – 41 to 45	35 ºC	with compensation

Figure 2 shows the four points where temperature measurements were taken on the parts inside the machining center, two points on the combustion face (points #1 and #2) and two other points on the cover face (points #3 and #4).

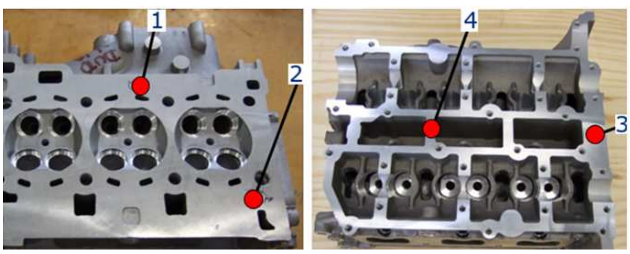

Figure 2. Workpiece used for machining tests with heated part and indication of temperature measurement points.

Workpiece temperature was measured at each tool change using an M&H 25.44 HDR temperature probe with 91.40-RX/TX infrared receiver (Figure 3).

Figure 3. Temperature probe M&H 25.44 HDR.

The previous pieces heating was carried out by storing them in an electric oven with temperature control (Figure 4). The pieces remained in the oven until they reached the pre-set temperature for the test.

Figure 4. Electric oven used for heating parts.

Thirteen cutting tools were used, including drills and countersinks, where 12 holes were machined. The machined holes that will later be measured in the CMM are: #3, #4, #11, #16, #17 and #18, as shown in Figure 5. In this work, the results obtained only for hole #3 will be presented.

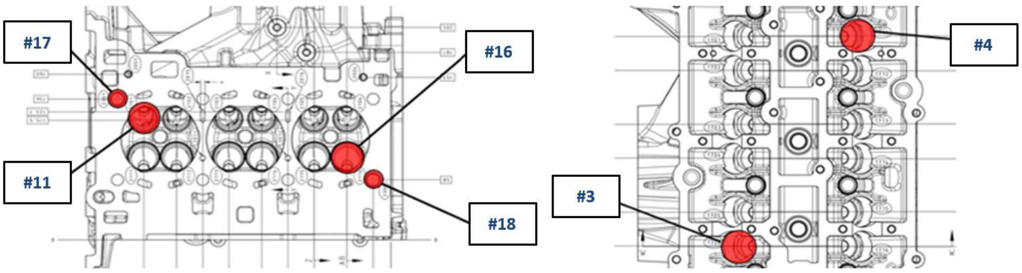

Figure 5. Holes measured in CMM.

2.2 Thermal Error Compensation Methodology

The compensation of thermal errors was conducted through the thermal compensation of the part, with a model based on the calculation of thermal compensation factors from the results obtained in the 1st and 2nd experimental steps, and directly inserted in the CNC program for each drilled hole. The model is validated by machining a new batch of parts in the 3rd step.

2.2.1 Methodology of workpiece thermal compensation

From the results obtained during the 1st and 2nd machining steps, the linear behavior of thermal errors was verified after measurements of the machined parts. Therefore, it was defined that the linear thermal expansion coefficient α would be determined from the calculation of the displacements between the average positions X and Y of the 5 pieces at 20 °C (reference) and of the 5 pieces at the upper temperature, for example 25 °C. The expansion coefficient is calculated through the linear relationship of thermal expansion given by Equation (1).

$$\alpha = \frac{\Delta l}{l_0 \cdot \Delta T} \quad (1)$$

where
α .... linear thermal expansion coefficient
ΔT .... temperature gradient
Δl .... linear thermal expansion
l_0 .... reference distance

The variable l_0 represents the average distance between the holes machined in the batch of 5 pieces at the temperature T1 = 20 ºC. The variable Δl is the difference in the average coordinate of a given characteristic between the parts machined at T1 = 20 ºC and the parts machined at the higher temperature, e.g. T2 = 25 ºC, that is, it represents the linear thermal expansion. Figure 6 schematically shows in (a) the presented variables, and in (b) illustrates a case of temperature variation ΔT obtained, after machining a given hole, through the "T" code of the cutting tool.

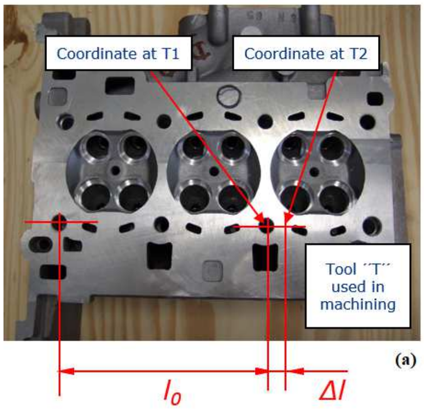

Tool code / Temperature	T_1 [°C]	T_2 [°C]	ΔT [°C]
Tool T_1	20.9	25.4	4.4
...	...	...	...
T_3	24.8	28.0	3.1
...	...	...	...
$T_{(final)}$	26.8	29.3	2.5

(b)

Figure 6. (a) Indication of reference distance l_0 and Δl, (b) illustration of ΔT determination.

3. RESULTS AND DISCUSSIONS

3.1 Thermal results from Step 1

Figure 7 shows the temperature results obtained in the first stage of the machining tests. Since only the temperature of the part was measured after machining tool T1 and the temperature after machining completion (after tool T13), the temperature behavior was assumed to be linear. The temperature was measured at points #3 and #4 on the cover face, and the result shown is the average value for the five pieces of each batch.

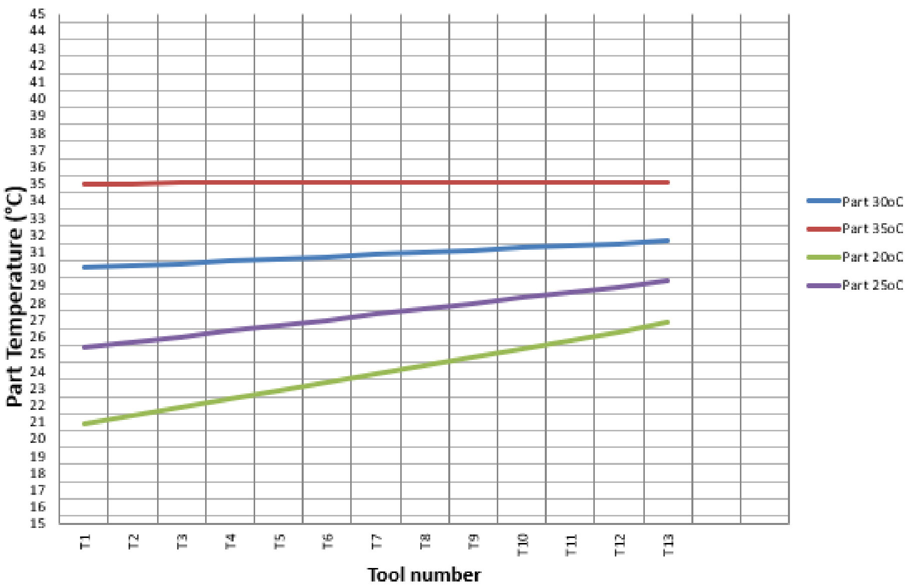

Figure 7. Thermal behavior of parts machined in step 1.

It can be seen in Figure 7 that the greatest temperature gradient occurred in the parts from batch #1, which entered the machine with the lowest temperature. In this group, the parts started at an average temperature of 20.9ºC after machining tool T1 and came out at 26.8ºC after machining tool T13, corresponding to an increase of 5.9ºC (28.2%) due to machining. For lot #2, where the parts started in the machine with an average temperature of 25.4ºC and came out at 29.3ºC, there was a delta of 3.9ºC, or 15.3% increase due to machining. As for batch #3, in which the parts started at a temperature of 30.0ºC, after the end of machining they were at 31.6ºC, therefore with a delta of 1.6ºC (5.3%). And finally, for batch #4, where the parts started in the machine at the highest temperature of 35.0ºC, the delta was the lowest of just 0.1ºC or 0.3%, with a final temperature equal to 35.1ºC. In this step, all 20 machined parts were measured.

3.2 Thermal results from Step 2

Figure 8 shows the temperature results obtained during the second stage machining tests. The combustion face, through points #1 and #2, was measured only after the changes of the last four tools (T10, T11, T12 and T13) for the sake of accessing the measuring probe during the cycle. The cover face, through points #3 and #4, was measured after each of the thirteen tool changes. Temperatures shown are averages. In this step, the parts were machined at the initial temperatures of 20°C and 30°C only.

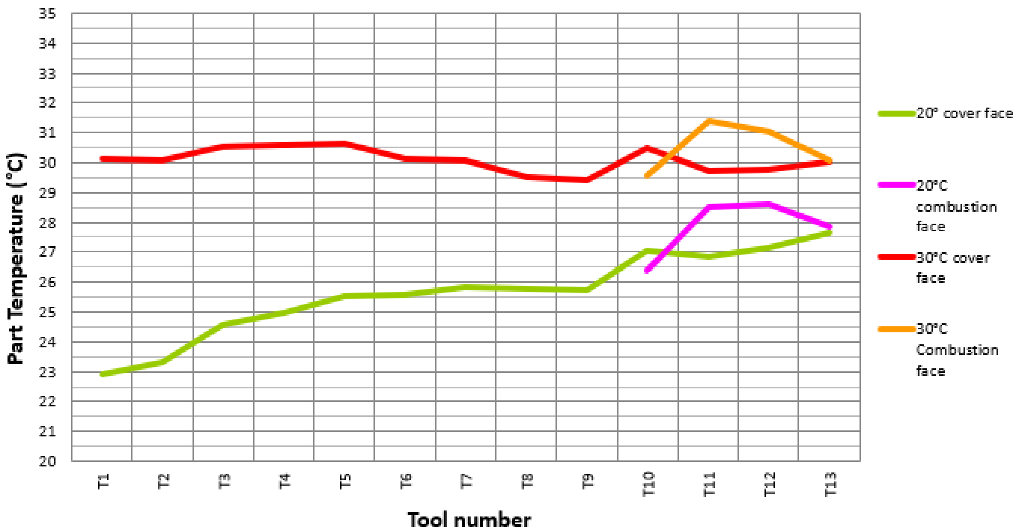

Figure 8. Thermal behavior of parts machined in step 2.

As can be seen in Figure 8, the temperature gradient at cover face for parts that entered the machine at a temperature of 20 ºC was 6.75 ºC (32.3%), values very close to the values obtained in the stage 1, which was 5.9 ºC.

Still in Figure 8, analyzing the temperature values read on the combustion face, there is a very small variation, in the order of 5%. This is mainly due to the proximity of the machined hole to the measured point. Analyzing now the temperature results obtained for the part entering the machine at a temperature of 30 ºC, it is again possible to conclude about a small, if not negligible, thermal influence of the machining, with gradients of less than 6% in the critical case in the comparison between the measurement of the cover face and the combustion face. Regarding the temperature difference between the part at the beginning and at the end of machining, it was less than 0.5 ºC.

Still analyzing the temperature results obtained during step 2, it is worth emphasizing the fact that the variations were smaller with the increase in the initial temperature of the part. It is also important to point out that the greatest heat contribution occurred due to the entry of tools T11 and T12, which raised the temperature by 2.1 ºC each in the parts with initial 20 °C temperature, which is justified by the greater removal of material and proximity of the machined holes of the measured points.

3.3 Thermal error measurements

After the parts were machined in the 1st and 2nd stages with different initial temperatures, they were all taken to the measuring room for measurement in a CMM of the hole position: #3. Based on the position deviation results obtained from these measurements, the thermal factors to compensate for thermal errors in real time in the machine will be determined.

The results of the X and Y coordinates of hole #3 for each of the 20 parts machined in step 1 will be presented below, considering the four inlet temperature variations: 20 ºC, 25 ºC, 30 ºC and 35 ºC.

Figure 9 shows a graph with the X coordinate values of the five parts for each temperature evaluated in step 1. The nominal coordinate in X is 39.750 mm with upper and lower limits ± 0.1 mm. The mean value of the 5 pieces in the test at 20 ºC was 39.618 mm, with a mean error in relation to the nominal value of 0.132 mm and standard deviation of 0.006 mm. In the test at 25 ºC, the mean value was 39.615 mm, with a mean error of 0.135 mm and standard deviation of 0.003 mm. As for the tests with the part initially at 30 ºC, the mean value of the coordinate in X was also 39.615 mm, the standard deviation was 0.004 mm with an average error of 0.135 mm. Finally, the test at 35 ºC obtained a mean coordinate of 39.596 mm, with a mean error in relation to the nominal equal to 0.154 mm and a standard deviation of 0.003 mm. The variation of the X coordinate of this characteristic in the different initial thermal conditions generated a maximum average error of 22 µm between the pieces in batch #1 in relation to the pieces of batch #4.

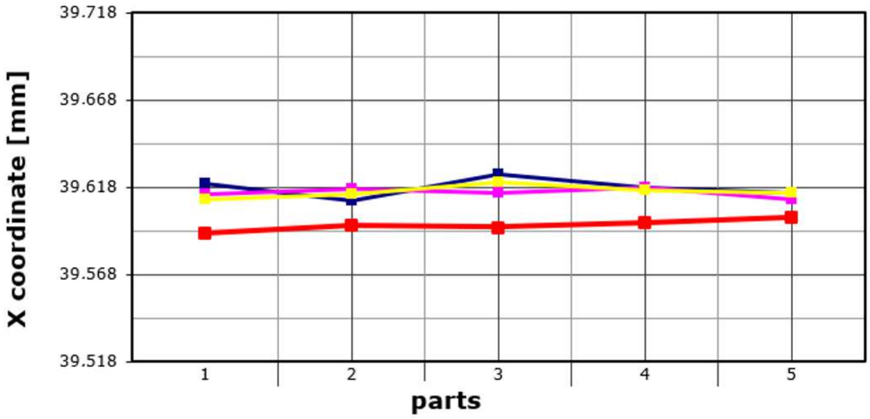

	1	2	3	4	5
20ºC	39.620	39.610	39.625	39.618	39.615
25ºC	39.614	39.617	39.615	39.618	39.611
30ºC	39.611	39.614	39.621	39.616	39.615
35ºC	39.592	39.596	39.595	39.598	39.601

Figure 9. Variation of the X coordinate of hole #3 (without compensation).

The nominal Y coordinate of hole #3 is 111.562 mm with upper and lower limits ± 0.1 mm. Figure 10 shows the plot of the Y coordinate of the five parts for each temperature evaluated. The mean value in the test at 20 ºC was 111.440 mm, with a mean error of 0.122 mm and standard deviation of 0.004 mm. In the test at 25 ºC, the mean value obtained by the measurement was 111,430 mm, with a mean error of 0.132 mm and standard deviation of 0.003 mm. For the tests with the part initially at 30 ºC, the mean value was 111.419 mm, the standard deviation was 0.001 mm with a mean error of 0.143 mm. Finally, the test at 35 ºC also obtained a mean coordinate of 111.419 mm, with mean error equal to 0.143 mm and standard deviation 0.004 mm. The variation of the Y coordinate of this characteristic in the different initial thermal conditions generated a maximum average error of 21 µm between the pieces in batch #1 in relation to the pieces of batch #4.

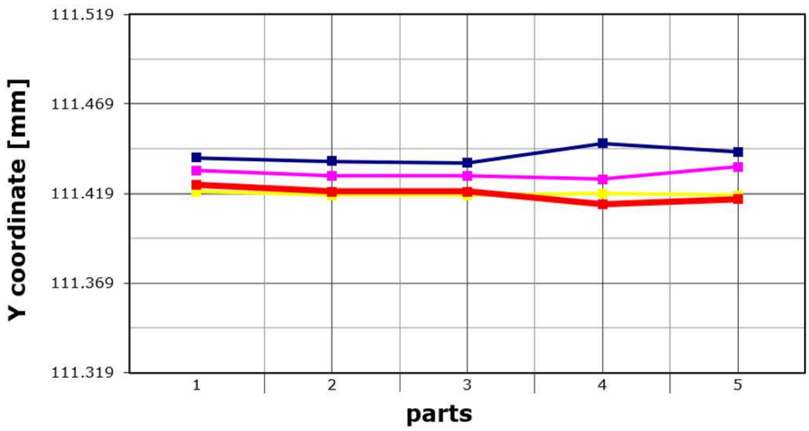

	1	2	3	4	5
20ºC	111.439	111.437	111.436	111.447	111.442
25ºC	111.432	111.429	111.429	111.427	111.434
30ºC	111.420	111.418	111.418	111.419	111.418
35ºC	111.424	111.420	111.420	111.413	111.416

Figure 10. Variation of the Y coordinate of hole #3 (without compensation).

3.4 Thermal Error Compensation Results

3.4.1 Thermal compensation of the workpiece

The thermal expansion coefficient was calculated for each machined feature, totaling 12 coefficients for the X coordinates and 12 for the Y coordinates. Figure 11 shows the values of the thermal expansion coefficient in the X direction calculated for each of the twelve machined features in the condition of part at 20 °C in relation to part at 25 °C.

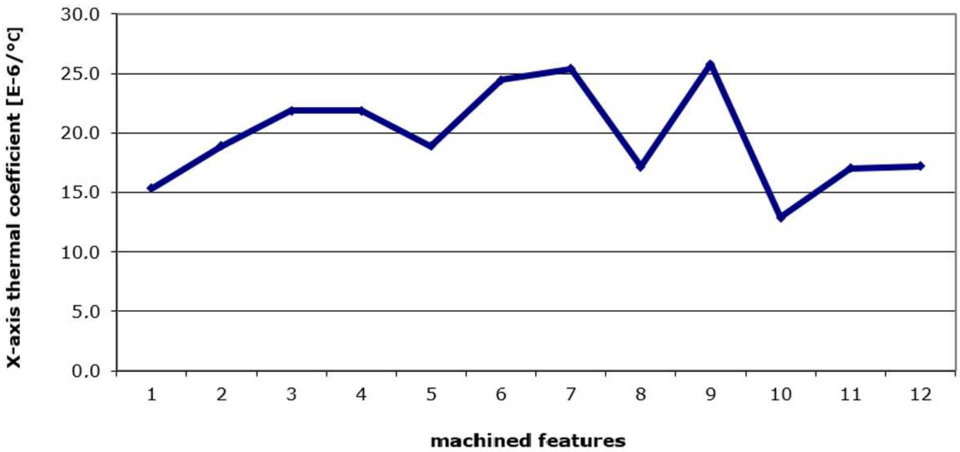

Figure 11. Thermal expansion coefficient in X direction for the 12 features machined into parts between 20 °C and 25 °C.

The thermal expansion coefficient calculated for all cases was between 12 and 38 [10^{-6}/K]. The mean value is 23.72 [10^{-6}/K]. If X and Y thermal expansion are analyzed separately, the coefficient to be adopted for X is 20.18 [10^{-6}/K] and for Y it would be equal to 27.25 [10^{-6}/K]. In this way the G code program was changed to consider the thermal expansion values.

3.4.2 Validation of the workpiece's thermal compensation model

For verification and validation of the proposed methodology, 15 pieces were machined in the 3rd step, divided into: 5 pieces at 25 °C with compensation, 5 pieces at 30 °C with compensation and 35 °C with compensation. All parts are measured in MMC to evaluate the X and Y coordinates of hole #3. As the machining center was not adjusted to guarantee the exact machining of the studied characteristics, the measurements obtained for the parts machined at 20 °C, without thermal compensation, were taken as a reference for evaluating the effectiveness after the implementation of the correction factors.

Figure 12 shows the comparative results obtained for the X coordinate of hole #3 for the 20 parts machined without compensation and 15 parts machined with compensation. The nominal X coordinate of hole #3 machined by tool T10 is 39.750 mm with upper and lower limits ± 0.1 mm. The average value obtained at the X coordinate for the workpiece at 20 °C temperature was 39.618 mm. As the machine was not adjusted to the nominal measurement, the value adopted as a reference was 39.618 mm.

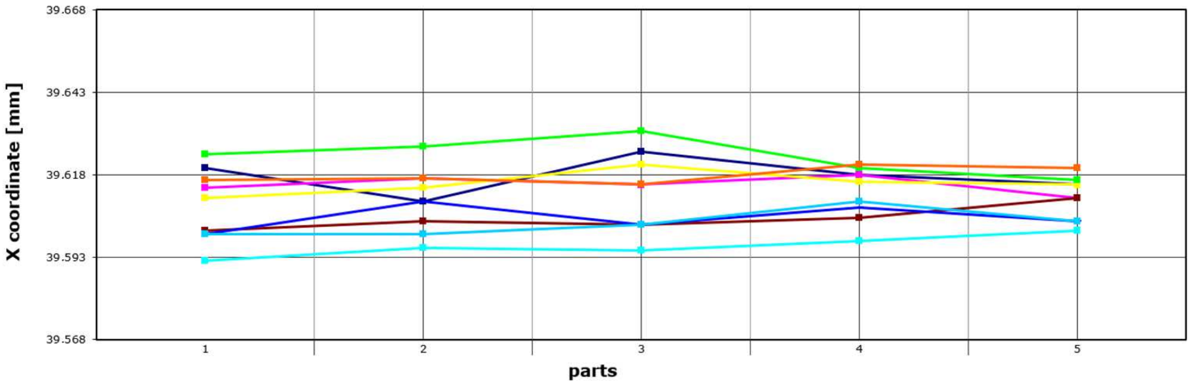

	1	2	3	4	5
20°C	39.620	39.610	39.625	39.618	39.615
25°C	39.614	39.617	39.615	39.618	39.611
30°C	39.611	39.614	39.621	39.616	39.615
35°C	39.592	39.596	39.595	39.598	39.601
25°C with comp	39.624	39.627	39.631	39.620	39.617
30°C with comp	39.601	39.604	39.603	39.605	39.611
35°C with comp	39.616	39.617	39.615	39.621	39.620

Figure 12. Comparison of the X coordinate of hole #3 (with and without compensation).

In the test at 25 ºC with compensation, the mean value measured was 39.624 mm, with a standard deviation of 0.006 mm. As for the tests with the part initially at 30 ºC with compensation, the mean value was 39.605 mm, and standard deviation was 0.004 mm. Finally, the test at 35 ºC with compensation obtained a mean coordinate of 39.618 mm, and a standard deviation of 0.003 mm. The variation of the X coordinate of this hole in the different initial thermal conditions generated a reduction in thermal errors of 22µm between the parts of lot #1 (reference parts at 20 °C) and the parts of lot #4 at 35 °C, which corresponds at 100% reduction.

Figure 13 shows the comparative results obtained for the Y coordinate of hole #3 for the 20 parts machined without compensation and 15 parts machined with compensation. The nominal Y coordinate of hole #3 is 111.562 mm with upper and lower limits ± 0.1 mm. The mean value obtained for this coordinate at 20 °C was 111.440 mm, and as the machine was not adjusted for the nominal measure, this mean measure was used as a reference in the analyses.

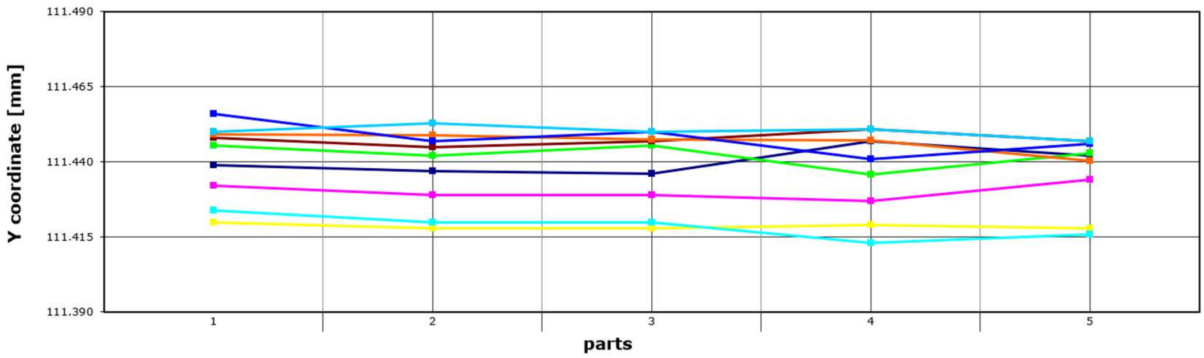

	1	2	3	4	5
20°C	111.439	111.437	111.436	111.447	111.442
25°C	111.432	111.429	111.429	111.427	111.434
30°C	111.420	111.418	111.418	111.419	111.418
35°C	111.424	111.420	111.420	111.413	111.416
25°C with comp	111.446	111.442	111.445	111.436	111.443
30°C with comp	111.448	111.445	111.447	111.451	111.447
35°C with comp	111.449	111.449	111.447	111.447	111.440

Figure 13. Comparison of the Y coordinate of hole #3 (with and without compensation).

In the test at 25 ºC with compensation, the mean value measured was 111.442 mm, and standard deviation 0.004 mm. For the tests with the part initially at 30 ºC with compensation, the mean value was 111.448 mm, with a standard deviation of 0.002 mm. Finally, the test at 35 ºC, with compensation, obtained a mean coordinate of 111.447 mm, with a standard deviation of 0.004 mm. The variation of the Y coordinate of this hole #3 in the different initial thermal conditions generated reductions in thermal errors between 62% and 80% between the parts of batch #1 (reference part at 20 °C) in relation to the parts of batch #4 at 35 °C.

4. CONCLUSIONS

After carrying out this research, it was possible to conclude that parts that entered the machine at an average temperature of 20 °C had their temperature increased by approximately 6 °C after machining, while parts that entered 25 °C increased by 4 °C, parts that entered 30 °C increased by only 2 °C, and the parts that entered the machine at 35 °C had practically no temperature variation after machining. The thermal errors obtained when comparing parts machined at 20 °C with parts machined at 35 °C reached 29 µm. This error is mainly due to the thermal expansion of the part, which occurred before it entered the machine. Analyzing the results obtained after the thermal compensation of the machined parts, it is possible to affirm that the developed methodology was effective, reducing thermal errors between 62% and 100%. The calculated thermal expansion coefficient encompasses both the thermal properties of the workpiece and the machining process (tools) and the machine itself, so the values were different from the thermal expansion coefficient of aluminum, normally close to 25x10-6/K, and varied significantly among themselves.

In future works the authors intend to carry out experiments considering the ambient temperature also varying, which should influence the thermoelastic behavior of the machine with consequences on the machined part.

5. ACKNOWLEDGEMENTS

The authors would like to acknowledge the companies B. GROB do Brazil and ESSS - ANSYS for their support in providing equipment and software.

6. REFERENCES

Abdulshahed, A.M., Longstaff, A. P., and Fletcher, S. “The application of ANFIS prediction models for thermal error compensation on CNC machine tools”. Applied Soft Computing Journal 27:158–68, 2015.

Delbressine, F. L. M., Florussen, G. H. J., Schijvenaars, L. A., and Schellekens, P. H. J. “Modelling thermomechanical behaviour of multi-axis machine tools”. Precision Engineering 30(1):47–53, 2006.

Li, Z.J., Zhao C.Y., and Lu, Z. C. “Thermal error modeling method for ball screw feed System of CNC machine tools in X-axis”. International Journal of Advanced Manufacturing Technology 106(11–12):5383–92, 2020.

Liu, C., Hrishikesh, V., Zhong, R.Y., and Xu X. “A systematic development method for cyber-physical machine tools”. Journal of Manufacturing Systems 48(March):13–24, 2018.

Mareš, M., Horejš, O., and Havlík, L. “Thermal error compensation of a 5-axis machine tool using indigenous temperature sensors and CNC Integrated Python code validated with a machined test piece”. Precision Engineering 66(July):21–30, 2020.

Miao, E.M., Ya, Y.G., Niu, P.C., Ji, C.Z., and Chen, H.D. “Robustness of thermal error compensation modeling models of CNC machine tools”. International Journal of Advanced Manufacturing Technology 69(9–12):2593–2603, 2013.

Ramesh, R., Mannan, M. A., and Poo, A.N. “Thermal error measurement and modelling in machine tools, Part I: Influence of varying operating conditions”. International Journal of Machine Tools and Manufacture 43(4):391–404, 2003.

Turek, P., Modrzycki, W., and Jędrzejewski, J. “Methods of machine tool error compensation”. Journal of Machine Engineering 10(4):5–25, 2010.

Xu, X. “Machine tool 4.0 for the new era of manufacturing”. International Journal of Advanced Manufacturing Technology 92(5–8):1893–1900, 2017.

Zhu, J., Ni, J., and Shih, A. J. "Robust Machine Tool Thermal Error Modeling Through Thermal Mode Concept." ASME. J. Manuf. Sci. Eng. 130(6), 2008.

7. RESPONSIBILITY NOTICE

The authors are the only responsible for the printed material included in this paper.